Article

*Discovery Medicine* 2025; 37(203): 3024–3035
https://doi.org/10.24976/Discov.Med.202537203.253

# LTBP3 Affects Acute Myocardial Infarction by Regulating Macrophage Polarization in Cardiac Fibroblasts

Huiying Sui[1], Lanchun Sun[1], Hongyu Rao[1], Tingting Sun[1], Liru Liu[1,*]

[1]Ward 5, Department of Cardiovascular Medicine, The Second Affiliated Hospital of Qiqihar Medical University, 161000 Qiqihar, Heilongjiang, China
*Correspondence: Liuliru@qmu.edu.cn (Liru Liu)
Submitted: 14 August 2025 Revised: 24 October 2025 Accepted: 28 October 2025 Published: 20 December 2025

**Background: Acute myocardial infarction (AMI) is a type of myocardial necrosis caused by acute ischemia or blood flow interruption in the coronary arteries, which poses a serious threat to human health. Activation of cardiac fibroblasts (CFs) and macrophage polarization play a crucial role in the pathogenesis of AMI. This study aims to elucidate the regulatory mechanisms between CFs and macrophage polarization during AMI progression.**

**Methods: RNA-seq data of AMI were downloaded for analysis. Differential expression analyses were performed on genes encoding secreted proteins, differentially expressed genes in single-cell infarct fibroblasts, and infarct tissues using the Human Protein Atlas (HPA) database. Differentially expressed genes *Latent transforming growth factor-$\beta$ binding protein 3* (*LTBP3*) and *podocan* (*PODN*) were analyzed in single-cell data comparing AMI samples with CFs, followed by receiver operating characteristic (ROC) analysis. LTBP3 and PODN protein expression was examined in a hypoxic cell model. LTBP3 recombinant protein was used to transfect macrophages, and the expression of CD16, CD86, iNOS, MHC-II, CD163, CD206, and arginase (Arg), as well as levels of *heparin-binding EGF-like growth factor* (*HBEGF*), *interleukin-1 beta* (*IL-1$\beta$*), *interleukin-6* (*IL-6*), and *tumor necrosis factor-$\alpha$* (*TNF-$\alpha$*), were assessed.**

**Results: A total of 11 cell types were identified through RNA-seq analysis, and 12 genes co-expressed across three datasets. Notably, *LTBP3* and *PODN* exhibited specifically high expression in myocardial infarction (MI) samples. Both *LTBP3* and *PODN* were significantly upregulated in MI, particularly in CFs ($p < 0.05$). Western blotting validated the upregulation of LTBP3 in CFs from MI samples compared with normal controls ($p < 0.05$), while PODN expression showed no significant difference in the AMI cell model relative to controls ($p > 0.05$). Co-immunoprecipitation (Co-IP) assay demonstrated that LTBP3 interacts with HBEGF. Overexpression of LTBP3 in CFs promoted macrophages polarization toward the M1 phenotype, as indicated by increased levels of M1 markers (CD16, CD86, iNOS, and MHC-II), and decreased levels of M2 markers (CD163, CD206, and Arg) ($p < 0.05$). Additionally, elevated HBEGF expression in macrophages enhanced the secretion of pro-inflammatory factors *IL-1$\beta$*, *IL-6*, and *TNF-$\alpha$* ($p < 0.05$). *HBEGF* knockdown reversed the effects of LTBP3-transfected CFs on macrophage differentiation and mitigated the inflammatory response, as evidenced by reduced *IL-1$\beta$*, *IL-6*, and *TNF-$\alpha$* levels ($p < 0.05$).**

**Conclusion: *LTBP3* in CFs modulates AMI progression by regulating macrophage polarization.**

**Keywords:** acute myocardial infarction; macrophage polarization; fibroblasts; LTBP3; HBEGF

## Introduction

Acute myocardial infarction (AMI) is myocardial necrosis caused by acute ischemia or blood flow interruption in the coronary arteries. The pathological remodeling of the heart muscle that occurs after myocardial infarction can trigger a series of adverse events, such as malignant arrhythmias, heart failure, and sudden death, all of which can affect the prognosis of patients with myocardial infarction and even threaten their life and health [1,2]. According to a 2025 report by the World Health Organization, cardiovascular diseases are the leading cause of death worldwide. In 2022, approximately 19.8 million people died from cardiovascular diseases, accounting for about 32% of the total global deaths. Of these, more than three quarters of cardiovascular disease deaths occurred in low- and middle-income countries [3]. Among these death cases, approximately half were caused by acute myocardial infarction due to coronary heart disease. Approximately one million individuals experience sudden AMI annually. Notably, one in every three patients with myocardial infarction (MI) succumbs to the condition, resulting in a mortality rate exceeding 3%. In recent years, there has been a trend toward younger onset ages, and the associated disease burden has become increasingly significant. AMI develops rapidly and has a poor prognosis, imposing a heavy medical and economic burden worldwide. Although the prognosis of MI has greatly improved with therapeutic strategies such as thrombolytic therapy and cardiac interventional proce-

dures, post-infarction ventricular remodeling still occurs in many patients, and many eventually progress to heart failure [4]. Thus, enhancing the focus on AMI and effectively managing the progression of ventricular remodeling are crucial for improving patient quality of life and reducing the incidence of AMI and heart failure.

Numerous studies have demonstrated that during MI, the synthesis and deposition of the extracellular matrix (ECM) persist in the infarcted region. ECM remodeling remains observable in this area for several years post-infarction, indicating a sustained activated state [5]. Cardiac fibroblasts (CFs) are essential for the formation of the myocardial ECM, with their proliferation and activation playing pivotal roles in the progression of myocardial fibrosis [6,7]. After MI, macrophages secrete a variety of factors, including transforming growth factor-$\beta$ (TGF-$\beta$), arginase-1 (Arg-1), and insulin-like growth factor-1 (IGF-1). The sustained secretion of these factors leads to the activation of CFs, which in turn influences macrophages and promotes their polarization. Cardiac macrophages are essential for cardiac inflammation, fibrotic remodeling, and tissue repair processes [8]. Investigating abnormalities in the number and function of polarized macrophages is essential for elucidating the mechanisms of AMI progression under stress conditions. Therefore, inhibition of CF activation and modulation of macrophage polarization may be critical for attenuating myocardial hyperfibrosis and adverse remodeling after MI. During myocardial infarction, whether CFs participate in regulating the polarization of macrophages and the key mechanisms underlying macrophage polarization mediated by CFs remain unclear.

Latent transforming growth factor-$\beta$ binding protein 3 (LTBP3) belongs to the family of latent TGF-$\beta$ binding proteins (LTBP), which contain modules such as the epidermal growth factor (EGF), the TGF-$\beta$ binding domain, cysteine-rich regions, a heterodimeric domain, and an EGF calcium-binding structural domain, which are structures similar to those of protofibrillar protein-I [9]. LTBP3 is highly expressed in various human tissues, including the ovary, prostate, adipose tissue, and heart. It has been shown that LTBP3 integrates into the extracellular matrix with the assistance of protofibrillar protein-I, and this process is impeded in the absence of protofibrillar protein-I *in vivo* or *in vitro*. Moreover, LTBP3 also plays a crucial role in the development and progression of various diseases, such as thoracic aortic aneurysm and skeletal dysplasia [10]. Moreover, LTBP3 is a key regulator of the TGF-$\beta$ signaling pathway [10]. LTBP family proteins has been observed in AMI patients and is positively correlated with AMI-related CFs [11], suggesting that LTBP3 may be a crucial factor in the pathophysiological mechanisms of AMI. Furthermore, LTBP3 is involved in regulating immune cell function and macrophage polarization [12]. Based on these findings, we hypothesize that CFs regulate macrophage polarization through LTBP3, thereby influencing the progression of MI.

This study aims to identify the key targets related to CFs and macrophages in the occurrence and development of AMI by analyzing sequencing data. Furthermore, combined with the cell co-culture techniques, it will explore the regulatory role of CFs in macrophage polarization during the pathophysiological progression of AMI and the related mechanisms. The aim of this study is to achieve a deeper understanding of the relationship between macrophage polarization and AMI and to provide a theoretical basis for further elucidating the underlying mechanisms of AMI occurrence and development.

## Materials and Methods

### *Sequencing Data Acquisition and Analysis*

The snRNA-seq data for MI were obtained from the Zenodo repository (https://zenodo.org/records/6578047), which includes processed single-nucleus RNA sequencing datasets stored in h5ad format. Prior to downstream analysis, the h5ad files were imported into the R environment using the Seurat package for data preprocessing. Quality control steps were applied to filter low-quality nuclei by removing those with $<$200 detected genes, $>$5% mitochondrial gene content, and $>$2000 total counts to exclude potential doublets or debris. Gene expression values were normalized, and logarithmic transformation was applied to reduce the influence of extreme values. Differential expression analysis of fibroblasts derived from myocardial infarction samples was conducted using the Limma package in R. Fibroblast abundance relative to *LTBP3* expression was quantified with the MCPcounter package. The correlation between *LTBP3* expression (log2-normalized counts) and fibroblast abundance scores was assessed using Pearson correlation analysis with the "cor.test" function, and results were visualized as scatter plots using the ggplot2 package. Quantification of M1-type and M2-type macrophage abundances was conducted using the quanTIseq package in R. All statistical analyses were performed in R (version 4.1.0, R Core Team).

### *Cell Acquisition and Culture*

Mouse CFs (JSY-CC2156) were purchased from Shanghai Jin Shaoyuan Biotechnology Co., Ltd. (Shanghai, China) and cultured in high-glucose Dulbecco's Modified Eagle's Medium (DMEM, C11995500BT, Gibco, Grand Island, USA) supplemented with 10% inactivated fetal bovine serum (FBS, 10099141C, Gibco, Grand Island, USA), 100 U/mL penicillin, and 100 g/mL streptomycin (SV30010, HyClone, USA). When cell confluence was $>$95%, the medium was replaced with serum-free DMEM, and hypoxic and normoxic control experiments were carried out after 24 h.

The mouse macrophage cell line RAW264.7 (authenticated by STR genotyping) was purchased from Peking University School of Medicine (Beijing, China) and cultured

in RPMI 1640 medium supplemented with 10% FBS, 100 U/mL penicillin, and 100 g/mL streptomycin at 37 °C in a humidified incubator (HERAcell 160i, Thermo scientific, Germany) containing 5% $CO_2$.

All cell lines used in the study, including primary cardiac fibroblasts and RAW264.7 macrophages, were tested for mycoplasma contamination using a PCR-based kit (MP0035, Sigma-Aldrich, MO, USA) at two critical stages: (a) prior to the initiation of experimental treatments, to ensure the absence of contamination in newly thawed or isolated cells; and (b) at 2-week intervals during long-term cell passage. All test results were negative, confirming the absence of mycoplasma contamination.

### *Construction of Hypoxic Cell Model*

CFs undergoing culture were placed in two vacuum desiccators, each with a volume of approximately 7 liters. These desiccators were separately ventilated with a gas mixture composed of 94% $N_2$, 5% $CO_2$, and 1% $O_2$ at a flow rate of 2 liters per minute for 15 minutes. This process ensured that the oxygen concentration within the desiccators reached 10-12%, which was maintained for 24 h to simulate hypoxic conditions. In contrast, normoxic control cells were cultured in a standard incubator continuously supplied with 5% $CO_2$ and air [13].

### *Co-Immunoprecipitation (Co-IP) Assay*

Pierce® Classic Magnetic IP/Co-IP Kit (3215115, ThermoFisher Scientific lnc., USA) was used to detect potential interacting proteins. RAW264.7 macrophages transduced with the siRNA-lentivirus were incubated for 48 h. The collected cells were lysed with RIPA buffer (P0013C, Beyotime, Shanghai, China) contain in a protease inhibitor cocktail (P1005, Beyotime, Shanghai, China) on ice for 30 min, following the manufacturer's protocol. The proteins in the cells were extracted and then the expression of target proteins and interacting proteins after gene silencing was detected by Western blotting.

### *Recombinant Protein Transfection and Verification*

CFs were plated into 6-well plates. When the cell density reached 60–80%, the cells were washed twice with Phosphate-Buffered Saline (PBS) (G0002, Servicebio, Wuhan, China), and 2 mL of serum-free medium (C0901, Beyotime, Shanghai, China) was added to each well. LTBP3 recombinant protein (RPro-LTBP3, CSB-YP889099HU, Huamei Bio) was then added for transfection. After gentle shaking and mixing, the cells were cultured in a 5% $CO_2$ incubator at 37 °C. After 24 h, the culture medium was aspirated and replaced with complete medium for further cultivation. After 3–4 days, the expression of related proteins was analyzed. To verify the transfection efficiency of the recombinant protein, western blotting was conducted to detect the protein expression of LTBP3 in CFs.

### *Co-Culture Experiment of CFs With RAW264.7 Macrophages*

The Transwell insert system (0.4 µm pore size, Corning) was used for the co-culture of CFs transfected with RPro-LTBP3 and RAW264.7 macrophages. CFs were seeded in the upper chamber ($5 \times 10^4$ cells/well), while RAW264.7 macrophages were seeded in the lower insert ($3 \times 10^4$ cells/well). Both cell types were cultured for 48 h, ensuring even distribution across each layer. The western blotting and PCR were conducted to detect the protein and mRNA expression levels of downstream target gene *HBEGF* of the gene *LTBP3* in macrophages. The macrophage polarization state was determined by assessing M1-type markers (CD16, CD86, iNOS, and MHC-II) and M2-type markers (CD163, CD206, and Arg) in both the control group and RPro-LTBP3 groups. Additionally, the expression levels of pro-inflammatory factors, including *IL-1*$\beta$, *IL-6*, and *TNF-*$\alpha$ were measured.

### *siRNA Transduction Effectively Downregulates the Expression of Critical Genes*

siRNA sequences targeting *HBEGF* were retrieved from established databases and literature, and subsequently designed. *HBEGF* siRNA was obtained from GenePharma (Shanghai, China). The siRNA sequence for mouse *HBEGF* was: sense, 5′-GGAGGUUAUGACUUGGAAAGU-3′; antisense, 5′-UUUCCAAGUCAUAACCUCCUC-3′. The control siRNA sequence was: sense, 5′-UUCUCCGAACGUGUCACGUTT-3′; and antisense, 5′-ACGUGACACGUUCGGAGAATT-3′. These siRNA sequences were cloned into appropriate lentiviral vectors. HEK293T cells were used to produce lentiviral particles, which were then added to the culture medium of RAW264.7 macrophages at a density of $5 \times 10^5$ cells/mL. Cells were maintained at 50–70% confluence during transduction to ensure a stable and controlled environment. RAW264.7 macrophages were transduced with the siRNA-lentivirus for 48 h. After transduction, knockdown efficacy was evaluated using RT-qPCR and western blot analysis. Total RNA and protein were isolated from RAW264.7 macrophages, and target gene expression levels were measured by RT-qPCR to confirm the siRNA efficacy. The macrophages were divided into three groups: control (untransfected), Si-ctrl group (transfected with control siRNA), and Si-HBEGF group (transfected with HBEGF siRNA). After 48 h of transfection, the polarization status, expression of inflammatory factors, and other relevant indicators were analyzed in each group.

### *Real-Time Quantitative Polymerase Chain Reaction (RT-qPCR)*

Total RNA was extracted from the cell samples using the kit reagents according to the manufacturer's instructions. Subsequently, RNA was reverse transcribed into

**Table 1. Sequences of the primers.**

| Gene | Forward primer, 5′-3′ | Reverse primer, 5′-3′ |
|---|---|---|
| *HBEGF* | ATCCTGCTGTTCTTCGGGTG | CCTTCCATGGGGACTGTGAC |
| *LTBP3* | AAGCAAGGACCATCTGCCTC | GGGGATCGAGTGTTGGTAGC |
| *IL-6* | GGGACTGATGCTGGTGACAA | CGCACTAGGTTTGCCGAGTA |
| *IL-1β* | GTCGCTCAGGGTCACAAGAA | CAAAGCAATGTGCTGGTGCT |
| *TNF-α* | ATGGCCTCCCTCTCATCAGT | ACCCTGAGCCATAATCCCCT |
| *β-actin* | CCACCATGTACCCAGGCATT | TCCTCTTAGGAGTGGGGGTG |

*HBEGF*, heparin-binding EGF-like growth factor ; *LTBP3*, *Latent transforming growth factor-β binding protein 3*; *IL-6*, interleukin-6; *IL-1β*, interleukin-1 beta; *TNF-α*, *tumor necrosis factor-α*.

cDNA using the BioScript All-in-One cDNA Synthesis SuperMix (Bimake, Houston, TX). RT-qPCR was conducted with the FastStart Universal SYBR Green Master Mix (Roche, Mannheim, Germany) on the CFX96 TM Real-Time PCR Detection System (Bio-Rad, Hercules, CA). Relative gene expression levels were calculated using the $2^{-(\Delta\Delta Ct)}$. The average threshold cycle (Ct) value for each transcript was normalized to $\beta$-actin. Primer sequences are provided in Table 1.

### *Western Blotting*

Cell lysates were prepared using RIPA buffer, and total proteins from each group were collected by centrifugation. Protein concentrations were determined using the BCA assay (P0012S, Beyotime, Shanghai, China). Equal amounts of protein from each sample were subjected to SDS-PAGE, and the separated proteins were transferred onto PVDF membranes using an electroblotting device. After transfer, the membranes were blocked with 5% fat-free milk in TBST (T1081, Solarbio, Beijing, China) for 1 h and then washed with TBST. The membranes were subsequently incubated overnight at 4 °C with the following primary antibodies: LTBP3 (1:500, A15687, Abclonal, China), PODN (1:500, 15014-1-AP, Proteintech, China), HBEFG (1:500, ab218019, Abcam, UK), CD16 (1:500, ab198507, Abcam, UK), CD86 (1:500, A16805, Abclonal, China), iNOS (1:1000, ab178945, Abcam, UK), MHC-II (1:500, ab139365, Abcam, UK), CD163 (1:1000, ab182422, Abcam, UK), CD206 (1:500, A21014, Abclonal, China), and Arg (1:5000, A25808, Abclonal, China). After primary antibody incubation, the membranes were washed and then incubated for 1 h with HRP-conjugated secondary antibodies: goat anti-rabbit IgG (1:2000, AS014, Abclonal, China) and goat anti-mouse IgG (1:2000, AS003, Abclonal, China). Protein bands were visualized using a chemiluminescence imaging system (ECL, 97-0827-02, Analytik Jena US, USA).

### *Statistical Analysis*

Statistical analyses were performed using GraphPad Prism9 software (version 9.4.1, LLC, Boston, MA, USA). Data are presented as mean ± standard deviation (SD). Statistical differences between two groups were assessed using the Student's *t*-test, while comparisons among multiple groups were performed using one-way ANOVA. When ANOVA indicated significance ($p < 0.05$), post hoc pairwise comparisons were conducted. A *p*-value less than 0.05 was considered statistically significant.

## Results

### *Bioinformatics Genetic Screen for MI*

To explore the pathogenesis of MI, we downloaded the snRNA-seq data of MI from Zenodo (https://zenodo.org/records/6578047) for analysis. A total of 11 cell subpopulations were identified, including vascular smooth muscle cells (vSMCs), pericytes, neurons, mast cells, macrophages, lymphoid cells, fibroblasts, endothelial cells, cycling cells, cardiomyocytes, and adipocytes (Fig. 1A). Secreted protein-coding genes were then obtained from the Human Protein Atlas (HPA, https://www.proteinatlas.org/) [14] and compared with the differentially expressed genes (DEGs) identified in single-cell infarct fibroblasts [15] ($p < 0.05$) and infarct tissues ($p < 0.05$, $\log|FC| > 1.5$). A total of 12 genes were found to be commonly expressed across all three datasets: *AEBP1*, *ANGPTL4*, *CCN1*, *COL14A1*, *COL1A1*, *COL1A2*, *COL5A1*, *LOXL2*, *LTBP2*, *LTBP3*, *PODN*, *THBS4* (Fig. 1B). Among these, 8 genes were highly expressed in fibroblasts, including *CCN1*, *COL1A1*, *COL1A2*, *COL5A1*, *LOXL2*, *LTBP2*, *LTBP3* and *PODN* (Fig. 1C). Notably, two genes, *LTBP3*, *PODN*, were specifically upregulated in CFs and have not been previously reported.

### *LTBP3 Was Significantly Upregulated in MI*

Bioinformatics analysis revealed that *LTBP3* was upregulated in MI ($t = -8.2938$, $p < 0.05$) (Fig. 2A). In addition, *LTBP3* was highly expressed in MI fibroblasts ($t = 8.0839$, df = 16616, $p < 0.05$) (Fig. 2B). *PODN* was also upregulated in MI ($t = -7.827$, $p < 0.05$) (Fig. 2C) and highly expressed in MI fibroblasts ($t = 7.3361$, df = 16427, $p < 0.05$) (Fig. 2D). Western blot and enzyme-linked immunosorbent assay (ELISA) for LTBP3 and PODN proteins were conducted in CFs and their supernatants using a hy-

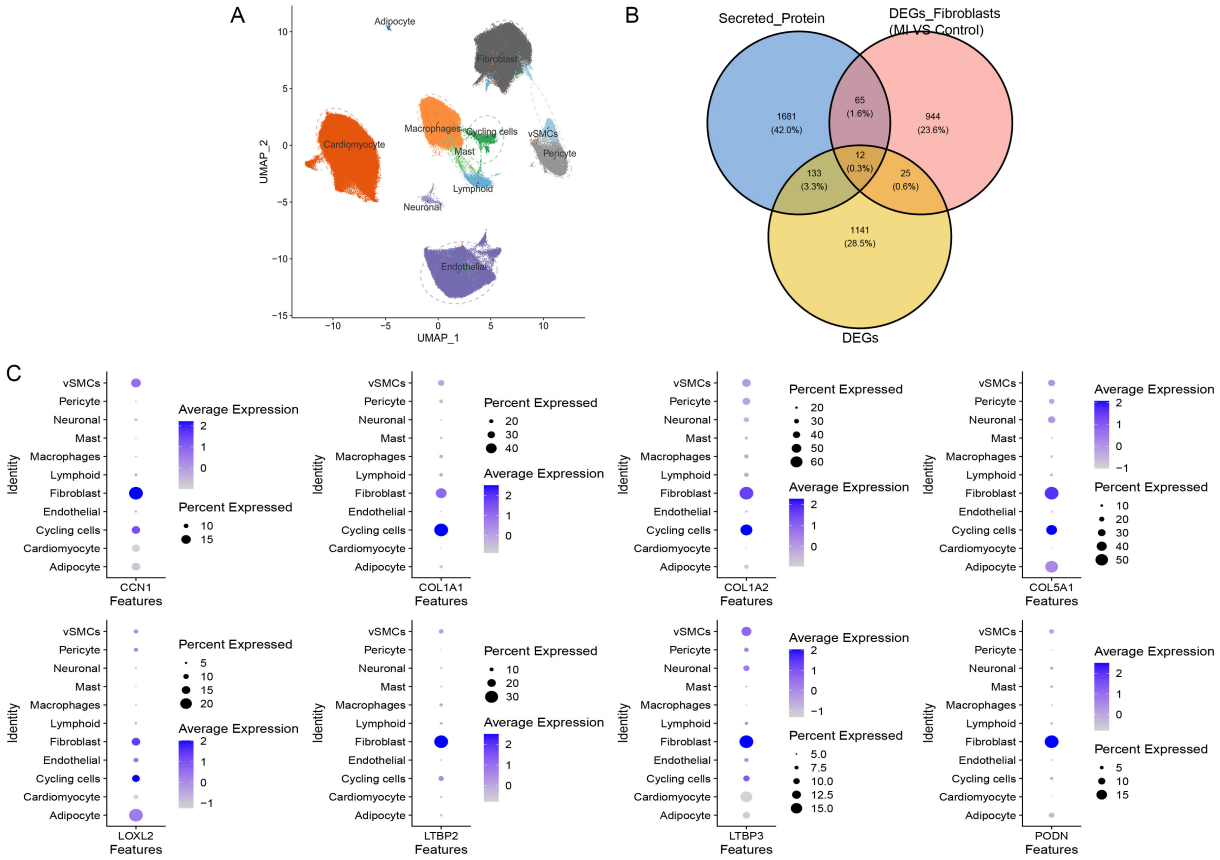


**Fig. 1. *LTBP3* and *PODN* are highly expressed in CFs from infarcted tissue.** (A) Uniform Manifold Approximation and Projection (UMAP) plot of single-cell MI data showing cell subpopulations. (B) Venn diagram of differentially expressed genes across analyzed datasets. (C) Dot plot illustrating high expression of *CCN1*, *COL1A1*, *COL1A2*, *COL5A1*, *LOXL2*, *LTBP2*, *LTBP3*, and *PODN*. *LTBP3*, *Latent transforming growth factor-β binding protein 3*; CFs, cardiac fibroblasts; MI, myocardial infarction.

poxic cell model. LTBP3 was significantly upregulated in the hypoxic cell model compared to the normal control in both cells and cell supernatants ($p < 0.05$), while there was no significant difference in PODN protein expression ($p > 0.05$) (Fig. 2E,F).

### *The Relationship Between LTBP3, CFs, and Macrophages During MI*

We investigated the relationship between *LTBP3*, CFs and macrophages during MI. First, cellchat analysis of single-cell data revealed that MI-associated fibroblasts mainly interacted most significantly with macrophages (Fig. 3A). Second, MCPcounter and quanTIseq immune infiltration analyses were performed on the GSE132143 gene expression matrix, revealing that *LTBP3* was positively correlated with fibroblast immune infiltration (R = 0.81, $p < 0.05$) (Fig. 3B), positively correlated with M1 cells (R = 0.752, $p < 0.05$) (Fig. 3C), and negatively correlated with M2 cells (R = –0.716, $p < 0.05$) (Fig. 3D). These findings indicate a significant correlation between elevated *LTBP3* expression and the polarization phenotype of macrophages during MI.

### *CFs Regulate Macrophage Polarization Through LTBP3*

The mechanism by which *LTBP3* regulates macrophage polarization in CFs was further explored. Single-cell analysis showed that HBEGF was highly expressed in macrophages from MI tissue (Fig. 4A). Results from Co-IP assays indicated that LTBP3 protein interact with HBEGF protein (Fig. 4B). The efficiency of RPro-LTBP3 transfection in CFs was verified, with expression levels of LTBP3 protein increased in the RPro-LTBP3 group ($p < 0.05$, Fig. 4C).

Co-culture of CFs transfected with RPro-LTBP3 with RAW264.7 macrophages resulted in significant upregulation of HBEGF protein and mRNA in the macrophages following exposure to RPro-LTBP3 ($p < 0.05$, Fig. 5A). In addition, the experimental results demonstrated that RAW264.7 macrophages in the RPro-LTBP3 group were polarized towards an M1 phenotype, characterized by elevated expression of M1 markers (CD16, CD86, iNOS, and MHC-II) and reduced expression of M2 markers (CD163, CD206, Arg) ($p < 0.05$, Fig. 5B). Moreover, in RAW264.7 macrophages, the inflammatory response was further en-

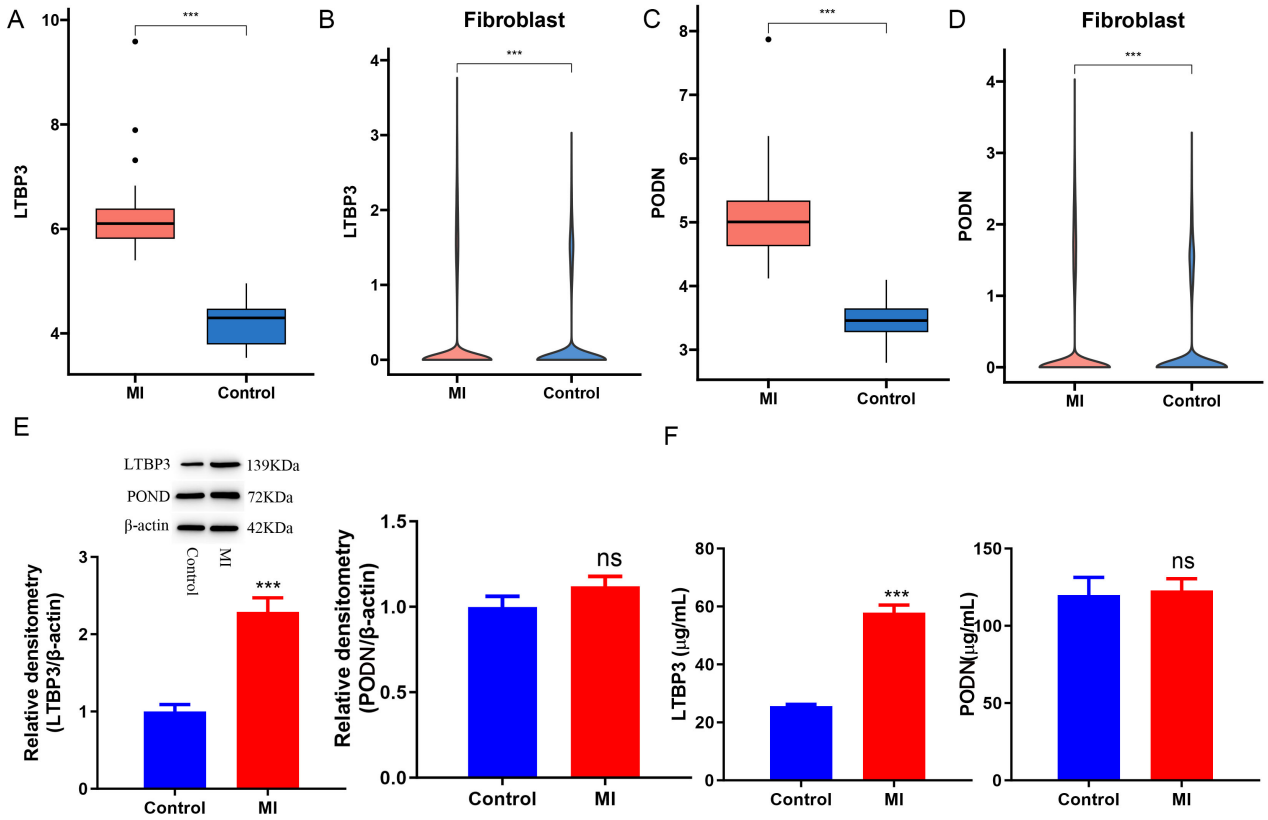


**Fig. 2. *LTBP3* was highly expressed in CFs from MI.** (A) Box plot of *LTBP3* differential gene analysis. (B) Violin plot of *LTBP3* in fibroblasts. (C) Box plot of *PODN* differential gene analysis. (D) Violin plot of *PODN* in fibroblasts. (E) Western blot assay for LTBP3 and PODN expression. (F) enzyme-linked immunosorbent assay (ELISA) of cell supernatant LTBP3 and PODN proteins expression. ***$p < 0.001$ *vs* control group; ns: the difference was not statistically significant.

hanced by the increased expression of HBEGF resulting from co-culture, which also led to increased expression of pro-inflammatory factors including *IL-1*$\beta$, *IL-6*, and *TNF-*$\alpha$ ($p < 0.05$, Fig. 5C–E). These findings suggest that HBEGF may serve as a critical downstream target of LTBP3 in promoting macrophage polarization.

### *LTBP3 Regulates Macrophage Polarization Through HBEGF*

We constructed *HBEGF* knockdown RAW264.7 macrophages, with RT-qPCR revealing a significant reduction in *HBEGF* mRNA expression in the Si-HBEGF group. Western blot analysis demonstrated a significant decrease in the protein expression levels of HBEGF in the same group ($p < 0.05$, Fig. 6A,B). Co-culture of CFs overexpressing *LTBP3* with HBEGF-knockdown RAW264.7 macrophages demonstrated that HBEGF knockdown significantly reversed the effect of *LTBP3* overexpression on macrophage polarization ($p < 0.05$, Fig. 6C), and also significantly reduced the expression of pro-inflammatory cytokines *IL-1*$\beta$, *IL-6*, and *TNF-*$\alpha$ ($p < 0.05$, Fig. 6D–F). The results of the pairwise comparisons among the groups were all obtained through post-hoc analysis.

## Discussion

AMI is a life-threatening condition characterized by the loss of myocardial tissue and an extremely limited regenerative capacity. Myocardial ischemia triggers cell death in the infarcted area, leading to the recruitment and activation of immune cells. This process sets off an inflammatory response in the early stages, followed by tissue repair and fibrosis. Following AMI, the majority of macrophages initially present in the infarcted area undergo apoptosis, and the region becomes predominantly populated by infiltrating neutrophils and monocyte-derived macrophages [16]. The migration and stimulation of these cells lead to a strong inflammatory reaction, secretion of cytokines, and subsequent cell death occurring promptly after AMI [17]. During tissue repair, the macrophage population in the infarcted region transitions from a pro-inflammatory to a pro-healing phenotype, facilitating collagen deposition, extracellular matrix remodeling, and fibrosis [18–20].

Macrophages are a crucial cell type in AMI, with their polarization state closely related to disease progression. In patients with AMI, macrophages present a state of polarization imbalance that can play a dual role in the process of cardiac repair: supporting tissue regeneration,

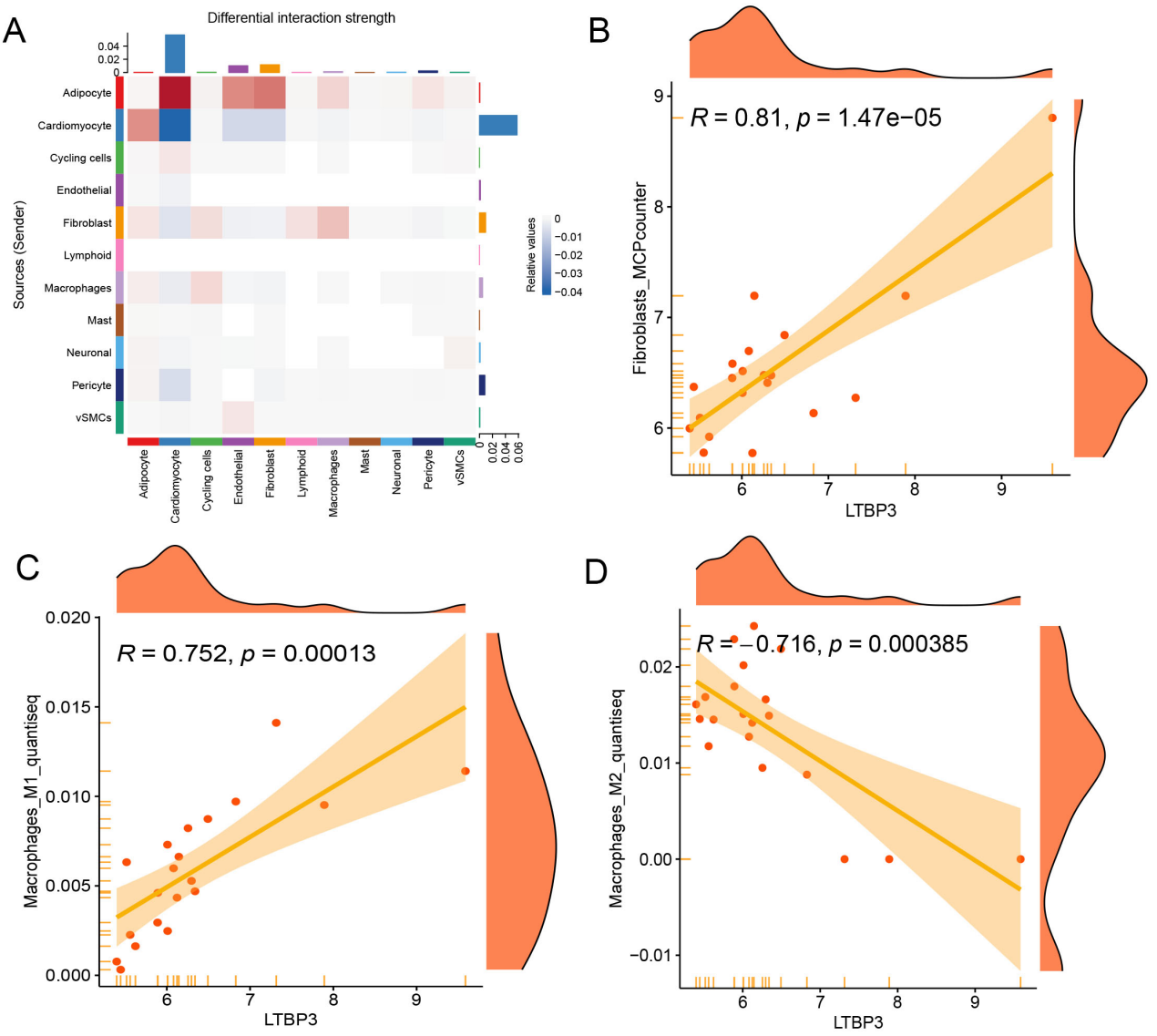


**Fig. 3. LTBP3 promotes macrophage polarization involved in MI processes.** (A) Cellchat analysis of MI single-cell data. (B) MCP counter between *LTBP3* and fibroblasts. (C) QuanTIseq analysis between *LTBP3* and M1-type macrophages. (D) QuanTIseq analysis between *LTBP3* and M2 type macrophages.

while also contributing to myocardial damage [21]. The intricate and dynamic phenotypic profile of macrophages following MI poses significant challenges for targeted therapies. A deeper understanding of the mechanisms governing macrophage phenotypic transitions in pathological contexts may inform the development of novel intervention strategies.

This study aimed to investigate LTBP3 expression changes in AMI fibroblasts and analyze its effect on macrophage polarization to elucidate its role in AMI pathogenesis and provide new mechanistic insights and therapeutic strategies. Bioinformatics analysis revealed that LTBP3 was significantly elevated in MI, indicating its strong discriminatory power and sensitivity for MI diagnosis. Correlation analysis of the GSE132143 gene dataset showed that *LTBP3* was positively correlated with fibroblasts and significantly positively correlated with macrophage M1 polarization and negatively correlated with macrophage M2 polarization. These findings suggest that CFs in MI mediate disease progression by regulating macrophage polarization through LTBP3, a key regulator of TGF-$\beta$.

The mechanism by which LTBP3, as a regulator of transcription factors, regulates the expression of downstream molecules, thus producing regulation of macrophage polarization, remains unknown. In order to explore the mechanisms, we conducted a Cellchat analysis. The research results revealed that fibroblasts related to acute infarction mainly interacted most signifi-

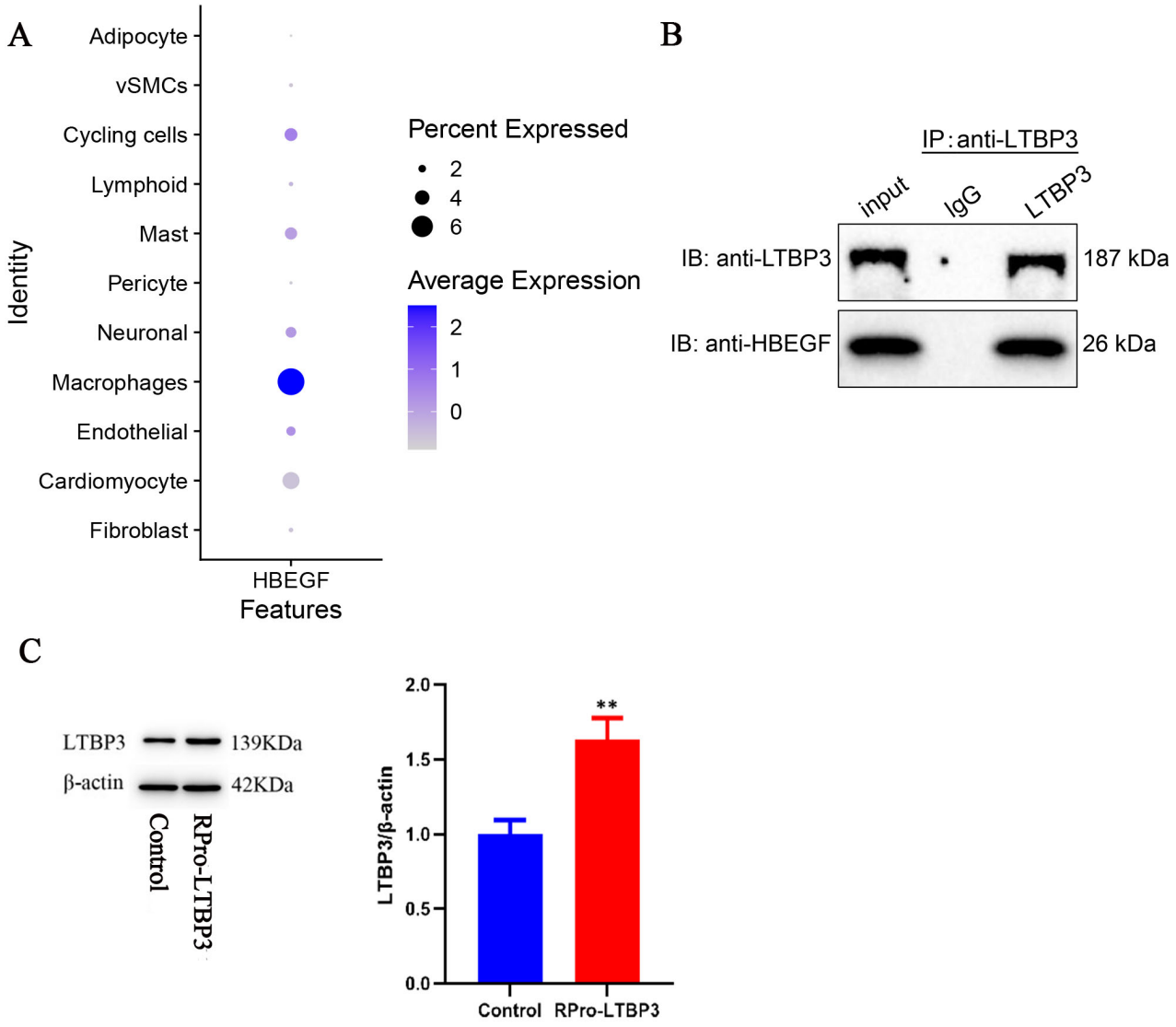


**Fig. 4. CFs promote HBEGF expression through LTBP3.** (A) Dot plot of HBEGF in macrophage cells. (B) Co-IP assay of LTBP3 with HBEGF. (C) Western blot assay of LTBP3 in CFs. $^{**}p < 0.01$ *vs* control group. Co-IP, Co-immunoprecipitation.

cantly with macrophages. To further elucidate the mechanism by which LTBP3 in CFs influences macrophage polarization and subsequently the progression of MI through the regulation of HBEGF, we conducted Co-IP assays, which confirmed the interaction between the *LTBP3* gene and the *HBEGF* gene. Our study also found that HBEGF was significantly positively correlated with macrophage polarization and the levels of LTBP3, suggesting that HBEGF might be a downstream target of LTBP3 and plays a crucial role in macrophage polarization.

HBEGF, a member of the EGF family with heparin-binding properties, was first identified in conditioned media derived from human macrophages. HBEGF and other EGF family members are initially produced as transmembrane proteins, including proHBEGF. These proteins can signal to receptors on adjacent cells or be released through proteolytic cleavage of their extracellular domains by metalloproteinases [22,23]. The secreted form can interact freely with receptors on the same cell or distant cells. The EGF family promotes receptor dimerization and autophosphorylation via the four HER/ErbB receptor tyrosine kinases, activating downstream signaling pathways that regulate diverse cellular processes [24]. Numerous studies have demonstrated that the expression of the *HBEGF* gene is tightly regulated by cytokines, transcription factors, and growth factors [25–27]. HBEGF is involved in physiolog-

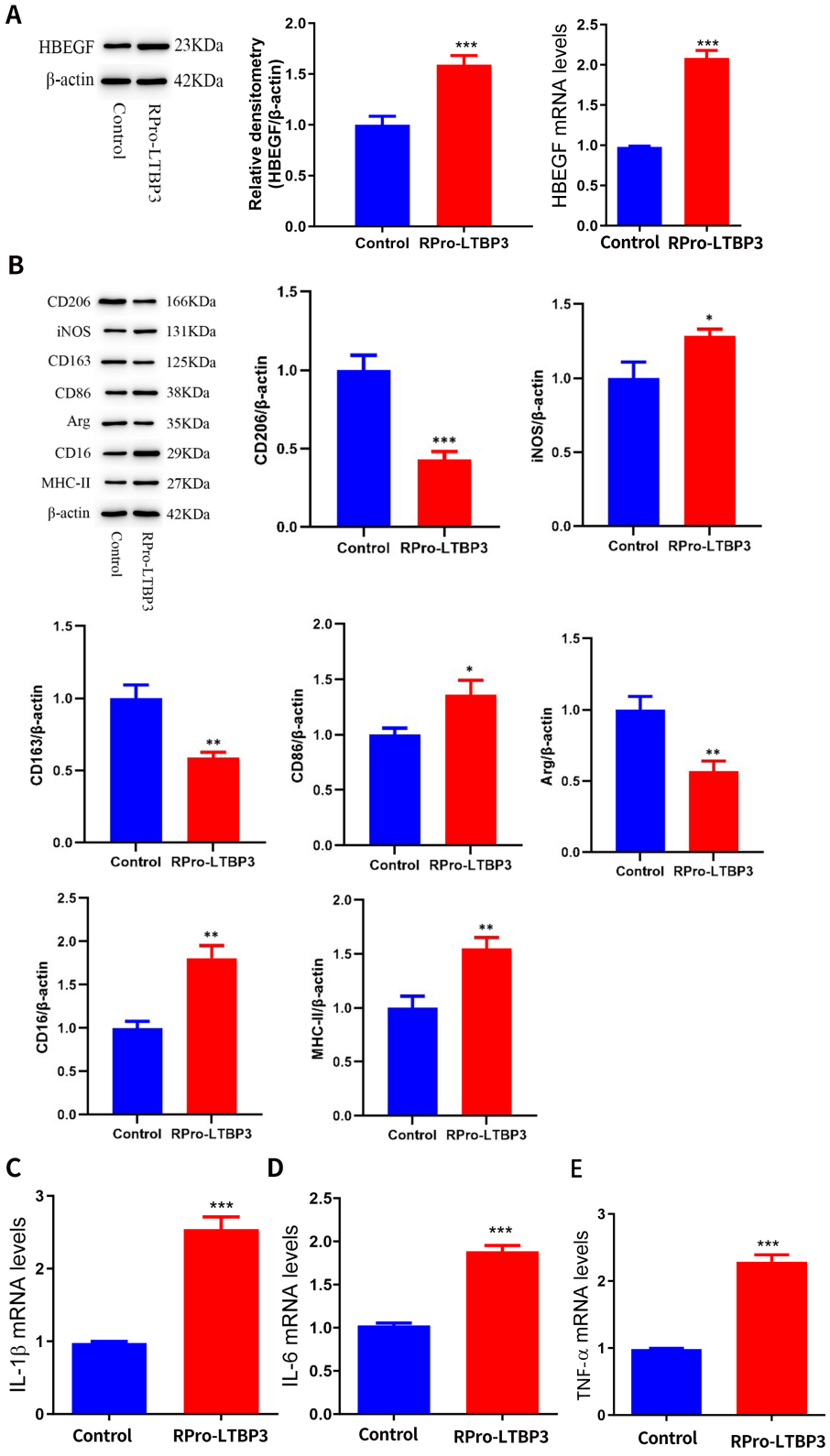


**Fig. 5. CFs regulate macrophage polarization through LTBP3.** (A) Western blot assay and the the RT-qPCR assay of HBEGF in the RPro-LTBP3 group. (B) Western blot assay of CD16, CD86, iNOS, MHC-II, CD163, CD206, and Arg in the RPro-LTBP3 group. (C) RT-qPCR of *IL-1β* in the RPro-LTBP3 group. (D) RT-qPCR of *IL-6* in the RPro-LTBP3 group. (E) RT-qPCR of *TNF-α* in the RPro-LTBP3 group. *$p < 0.05$ *vs* control group; **$p < 0.01$ *vs* control group; ***$p < 0.001$ *vs* control group.

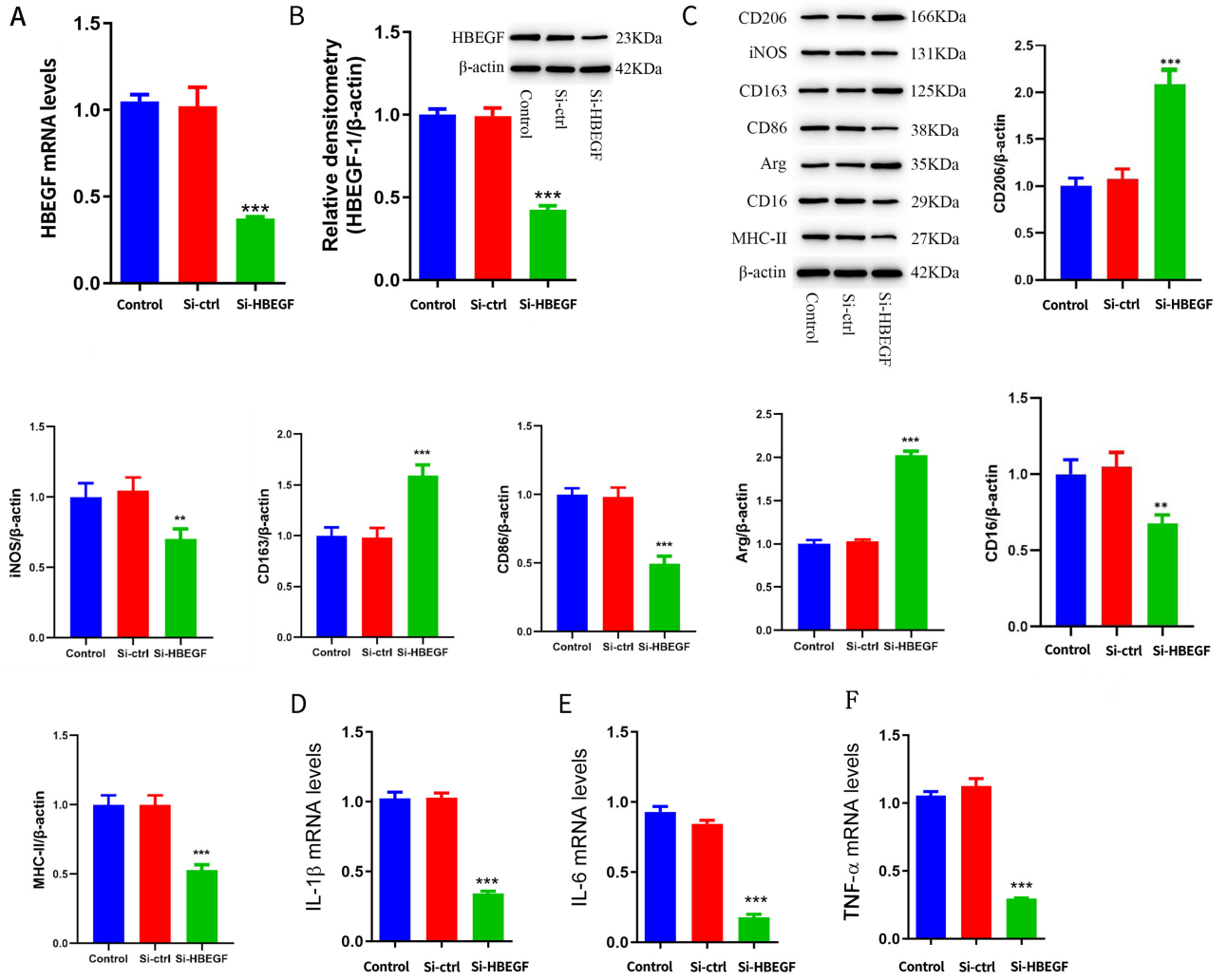


**Fig. 6. LTBP3 regulates macrophage polarization through HBEGF.** (A) RT-qPCR assay of HBEGF in the Si-HBEGF group. (B) Western blot assay of HBEGF in the same group. (C) Western blot assay of CD16, CD86, iNOS, MHC-II, CD163, CD206, and Arg in the macrophage RAW264.7 macrophages transfected with Si-HBEGF, both prior to and following co-culture. (D–F) RT-qPCR assay of IL-1$\beta$, IL-6, TNF-$\alpha$, in the Si-HBEGF group. **$p < 0.01$ *vs* control group; ***$p < 0.001$ *vs* control group.

ical processes such as blastocyst implantation and wound healing, as well as pathological conditions including tumor progression, smooth muscle cell proliferation, and atherosclerosis [25]. Recent research has demonstrated that HBEGF plays a crucial role in regulating the pathophysiology of AMI. Additionally, AMI is closely related to the positive regulation of vascular-related smooth muscle cell proliferation and the production of cytokines involved in immune responses. HBEGF plays a crucial role in this process [28]. Specifically, HBEGF facilitates the production and activation of M1-type macrophages, exacerbating the inflammatory response in AMI. Conversely, the overexpression of HBEGF suppresses the production and activation of M2-type macrophages, thereby exacerbating the inflammatory response in AMI. Through sequencing analysis and *in vitro* experiments, our study found that inhibiting HBEGF expression may weaken M1-type macrophage polarization and regulate macrophage polarization overall. This suggests that HBEGF plays an important role in the treatment of acute myocardial infarction, providing a new direction for research on the treatment of acute myocardial infarction.

This study has some limitations. First, the conclusions have not been further validated *in vivo*. Future work will involve constructing gene knockout mouse models to strengthen the mechanistic evidence. Second, although co-immunoprecipitation confirmed the interaction between LTBP3 and HBEGF, the specific molecular mechanisms underlying this interaction require further investigation.

## Conclusion

In summary, during the pathophysiological process of AMI, HBEGF modulates macrophage polarization, influencing disease progression. Bioinformatic analyses indicate that LTBP3, acting as a transcription factor regulator, can bind to HBEGF targets. Consequently, LTBP3 is considered a critical upstream regulator of macrophage polarization through modulation of HBEGF expression, ultimately influencing the occurrence and development of AMI. These findings provide novel insights into AMI pathogenesis and contribute to the development of targeted therapies for AMI treatment.

## Availability of Data and Materials

The data that support the findings of this study are available from the corresponding author upon reasonable request.

## Author Contributions

HYS and LRL designed the research study; LCS, HYR and TTS performed the research; LCS, HYR and TTS collected and analyzed the data. HYS and LRL have been involved in drafting the manuscript and all authors have been involved in revising it critically for important intellectual content. All authors gave final approval of the version to be published. All authors have participated sufficiently in the work to take public responsibility for appropriate portions of the content and agreed to be accountable for all aspects of the work in ensuring that questions related to its accuracy or integrity.

## Ethics Approval and Consent to Participate

Not applicable.

## Acknowledgment

Not applicable.

## Funding

This study was funded by Basic Research of Undergraduate Colleges and Universities in Heilongjiang Province (2024-KYYWF-0362).

## Conflict of Interest

The authors declare no conflict of interest.

## References

[1] Byrne RA, Rossello X, Coughlan JJ, Barbato E, Berry C, Chieffo A, *et al*. 2023 ESC Guidelines for the management of acute coronary syndromes. European Heart Journal. 2023; 44: 3720–3826. https://doi.org/10.1093/eurheartj/ehad191.

[2] Wang R, Tu S, Tan M, Gao L. Clinical Risk Factors and Characteristics of Coronary Artery Lesions in Premature Acute Myocardial Infarction Patients. Discovery Medicine. 2024; 36: 2253–2263. https://doi.org/10.24976/Discov.Med.202436190.207.

[3] World Health Organization. Cardiovascular diseases (CVDs). 2025. Available at: https://www.who.int/news-room/fact-sheets/detail/cardiovascular-diseases-(cvds)#:~:text=An%20estimated%2019.8%20million%20people%20died%20from%20CVDs,85%25%20were%20due%20to%20heart%20attack%20and%20stroke (Accessed: 10 October 2025).

[4] Frantz S, Hundertmark MJ, Schulz-Menger J, Bengel FM, Bauersachs J. Left ventricular remodelling post-myocardial infarction: pathophysiology, imaging, and novel therapies. European Heart Journal. 2022; 43: 2549–2561. https://doi.org/10.1093/eurheartj/ehac223.

[5] Frangogiannis NG. The extracellular matrix in myocardial injury, repair, and remodeling. The Journal of Clinical Investigation. 2017; 127: 1600–1612. https://doi.org/10.1172/JCI87491.

[6] Wu X, Reboll MR, Korf-Klingebiel M, Wollert KC. Angiogenesis after acute myocardial infarction. Cardiovascular Research. 2021; 117: 1257–1273. https://doi.org/10.1093/cvr/cvaa287.

[7] Maimaitijiang A, Huang Q, Wu Y, Sun S, Chen Q. Transglutaminase 2 inhibition ameliorates cardiac fibrosis in myocardial infarction by inducing M2 macrophage polarization in vitro and in vivo. CytoJournal. 2024; 21: 58. https://doi.org/10.25259/Cytojournal_32_2024.

[8] Yap J, Irei J, Lozano-Gerona J, Vanapruks S, Bishop T, Boisvert WA. Macrophages in cardiac remodelling after myocardial infarction. Nature Reviews. Cardiology. 2023; 20: 373–385. https://doi.org/10.1038/s41569-022-00823-5.

[9] Carpenter G, Wahl MI. The epidermal growth factor family. In Sporn MB, Roberts AB (eds.) Handbook of Experimental Pharmacology (pp. 69–171). Springer-Verlag: New York. 1990.

[10] Robertson IB, Horiguchi M, Zilberberg L, Dabovic B, Hadjiolova K, Rifkin DB. Latent TGF-$\beta$-binding proteins. Matrix Biology: Journal of the International Society for Matrix Biology. 2015; 47: 44–53. https://doi.org/10.1016/j.matbio.2015.05.005.

[11] Chan MY, Efthymios M, Tan SH, Pickering JW, Troughton R, Pemberton C, *et al*. Prioritizing Candidates of Post-Myocardial Infarction Heart Failure Using Plasma Proteomics and Single-Cell Transcriptomics. Circulation. 2020; 142: 1408–1421. https://doi.org/10.1161/CIRCULATIONAHA.119.045158.

[12] Dabovic B, Chen Y, Choi J, Davis EC, Sakai LY, Todorovic V, *et al*. Control of lung development by latent TGF-$\beta$ binding proteins. Journal of Cellular Physiology. 2011; 226: 1499–1509. https://doi.org/10.1002/jcp.22479.

[13] Pavlacky J, Polak J. Technical Feasibility and Physiological Relevance of Hypoxic Cell Culture Models. Frontiers in Endocrinology. 2020; 11: 57. https://doi.org/10.3389/fendo.2020.00057.

[14] Salehi O, Mack H, Colville D, Lewis D, Savige J. Ocular manifestations of renal ciliopathies. Pediatric Nephrology (Berlin, Germany). 2024; 39: 1327–1346. https://doi.org/10.1007/s00467-023-06096-5.

[15] Kuppe C, Ramirez Flores RO, Li Z, Hayat S, Levinson RT, Liao X, *et al*. Spatial multi-omic map of human myocardial infarction. Nature. 2022; 608: 766–777. https://doi.org/10.1038/s41586-022-05060-x.

[16] Jia D, Chen S, Bai P, Luo C, Liu J, Sun A, *et al*. Cardiac Resident Macrophage-Derived Legumain Improves Cardiac Repair by Promoting Clearance and Degradation of Apoptotic Cardiomyocytes After Myocardial Infarction. Circulation. 2022; 145: 1542–1556. https://doi.org/10.1161/CIRCULATIONAHA.121.057549.

[17] Cai S, Zhao M, Zhou B, Yoshii A, Bugg D, Villet O, *et al*. Mitochondrial dysfunction in macrophages promotes inflammation and suppresses repair after myocardial infarction. The Journal of Clinical Investigation. 2023; 133: e159498. https://doi.org/10.1172/JCI159498.

[18] Sack MN. Mitochondrial fidelity and metabolic agility control immune cell fate and function. The Journal of Clinical Investigation. 2018; 128: 3651–3661. https://doi.org/10.1172/JCI120845.

[19] Wang X, Yang G, Li J, Meng C, Xue Z. Dynamic molecular signatures of acute myocardial infarction based on transcriptomics and metabolomics. Scientific Reports. 2024; 14: 10175. https://doi.org/10.1038/s41598-024-60945-3.

[20] Sun Q, Chen W, Wu R, Tao B, Wang P, Sun B, *et al*. Serine protease inhibitor, SerpinA3n, regulates cardiac remodelling after myocardial infarction. Cardiovascular Research. 2024; 120: 943–953. https://doi.org/10.1093/cvr/cvae075.

[21] Rizzo G, Gropper J, Piollet M, Vafadarnejad E, Rizakou A, Bandi SR, *et al*. Dynamics of monocyte-derived macrophage diversity in experimental myocardial infarction. Cardiovascular Research. 2023; 119: 772–785. https://doi.org/10.1093/cvr/cvac113.

[22] Jessmon P, Leach RE, Armant DR. Diverse functions of HBEGF during pregnancy. Molecular Reproduction and Development. 2009; 76: 1116–1127. https://doi.org/10.1002/mrd.21066.

[23] Chen N, Fan B, He Z, Yu X, Wang J. Identification of HBEGF+ fibroblasts in the remission of rheumatoid arthritis by integrating single-cell RNA sequencing datasets and bulk RNA sequencing datasets. Arthritis Research & Therapy. 2022; 24: 215. https://doi.org/10.1186/s13075-022-02902-x.

[24] Holbro T, Hynes NE. ErbB receptors: directing key signaling networks throughout life. Annual Review of Pharmacology and Toxicology. 2004; 44: 195–217. https://doi.org/10.1146/annurev.pharmtox.44.101802.121440.

[25] Raab G, Klagsbrun M. Heparin-binding EGF-like growth factor. Biochimica et Biophysica Acta. 1997; 1333: F179–F199. https://doi.org/10.1016/s0304-419x(97)00024-3.

[26] Oyagi A, Oida Y, Kakefuda K, Shimazawa M, Shioda N, Moriguchi S, *et al*. Generation and characterization of conditional heparin-binding EGF-like growth factor knockout mice. PloS One. 2009; 4: e7461. https://doi.org/10.1371/journal.pone.0007461.

[27] Su Y, Besner GE. Heparin-binding EGF-like growth factor (HB-EGF) promotes cell migration and adhesion via focal adhesion kinase. The Journal of Surgical Research. 2014; 189: 222–231. https://doi.org/10.1016/j.jss.2014.02.055.

[28] Wang Y, Xian H. Identifying Genes Related to Acute Myocardial Infarction Based on Network Control Capability. Genes. 2022; 13: 1238. https://doi.org/10.3390/genes13071238.